

Xuan Liu

The Combustion Laboratory,
Department of Mechanical Engineering,
University of Maryland,
College Park, MD 20742;
State Key Laboratory of Multiphase
Flow in Power Engineering,
School of Energy and
Power Engineering,
Xi'an Jiaotong University,
Xi'an 710049, China
e-mail: liuxuanne@foxmail.com

Kiran Raj G. Burra

The Combustion Laboratory,
Department of Mechanical Engineering,
University of Maryland,
College Park, MD 20742
e-mail: kiranraj@umd.edu

Zhiwei Wang

The Combustion Laboratory,
Department of Mechanical Engineering,
University of Maryland,
College Park, MD 20742;
College of Environmental Engineering,
Henan University of Technology,
Zhengzhou 450001, China
e-mail: bioenergy@163.com

Jinhu Li

The Combustion Laboratory,
Department of Mechanical Engineering,
University of Maryland,
College Park, MD 20742;
School of Safety Engineering,
China University of Mining and Technology,
Xuzhou 221116, China
e-mail: ljh_cumt@163.com

Defu Che

State Key Laboratory of Multiphase
Flow in Power Engineering,
School of Energy and
Power Engineering,
Xi'an Jiaotong University,
Xi'an 710049, China
e-mail: dfche@mail.xjtu.edu.cn

Ashwani K. Gupta¹

The Combustion Laboratory,
Department of Mechanical Engineering,
University of Maryland,
College Park, MD 20742
e-mail: ak Gupta@umd.edu

Influence of Char Intermediates on Synergistic Effects During Co-Pyrolysis of Pinewood and Polycarbonate

Combined use of plastic and biomass wastes offers promising pathway for simultaneous energy production and waste disposal. In this article, the co-pyrolysis of pinewood and polycarbonate (PC) was performed in a fixed bed reactor to quantify their synergistic interaction on the product output and determine the effect of char intermediates on the synergistic effects. The extent of synergistic effects was obtained via a direct comparison of results from co-pyrolysis of pinewood–polycarbonate mixture with the weighted average values from pyrolysis of individual components. The observed synergistic effects were further examined from the influence of char intermediates using tailored feedstock configurations to gain more insights into the synergistic mechanism. The results showed co-pyrolysis resulted in enhancement by 33% in H_2 , 26% in CO , and 19% in total syngas yields compared to their weighted values from individual pyrolysis. Co-pyrolysis also exhibited superiority in energy recovery with the overall energy efficiency promoted from 42.9% to 48.6%. Deconvolution of synergistic effects revealed that pinewood char catalytically enhanced PC degradation, while the effect of PC char on pinewood pyrolysis was minimal. This article provides results on deconvolved understanding of synergistic effects in co-pyrolysis of lignocellulosic biomass and PC wastes, which is very helpful in designing clean and efficient energy recovery systems from these waste resources. [DOI: 10.1115/1.4049464]

Keywords: lignocellulosic biomass, waste polycarbonate, co-pyrolysis, synergistic effects, feedstock configuration, alternative energy sources, energy conversion/systems, energy extraction of energy from its natural resource, energy from biomass

1 Introduction

Energy Outlook 2020 by the British Petroleum (BP) Company cites that the world energy demand is expected to increase by

some 33% in the next 20 years to support the growing population and rapid urbanization [1]. These growing energy demands need to be met by developing sustainable and versatile energy solutions based on renewable resources while also recovering waste materials to decrease the net greenhouse gas emissions and establishing circular utilization of these energy resources for carbon neutral operation. Biomass comprises mainly forestry wood, agricultural residues, and energy crops, which is an ideal renewable energy resource with abundant availability of around 100 billion metric tons per year [2] and short carbon cycle to provide recyclable carbonaceous

¹Corresponding author.

Contributed by the Advanced Energy Systems Division of ASME for publication in the JOURNAL OF ENERGY RESOURCES TECHNOLOGY. Manuscript received November 27, 2020; final manuscript received December 3, 2020; published online January 27, 2021. Editor: Hameed Metghalchi.

resource to derive carbon based energy, fuels, and chemicals compatible with existing fossil fuel infrastructure [3]. However, these biomass resources (especially lignocellulosic biomass from forestry and agricultural residues) are subject to seasonal availability issues and thus require other supplementary feedstocks for sustainable and stable energy output throughout the year.

Plastics are fossil fuel-derived materials but have become indispensable in the modern society. Among these various synthetic polymers, bisphenol A polycarbonate (PC) is a commonly used plastic due to its high impact strength, excellent thermal resistance, and superior electrical insulation properties, and often finds greater use in building and construction, automobile industry, and data storage devices (such as compact discs) [4,5]. Global PC production has steadily increased over the recent past, reaching 6 million metric tons in 2017 [6]. However, only a small portion (around 7%) of the produced PC was recycled leading to significant amounts of PC being land-filled [7]. Landfilling as a disposal pathway is not sustainable since PC wastes are nonbiodegradable, and all land resources are limited in addition to environmental concerns of leaching of bisphenol A, which is identified as an endocrine disruptor and can induce a series of adverse effects on the ecosystem and human health [8]. Furthermore, from the perspective of energy recovery, landfilling PC wastes results in a remarkable loss of potential fossil fuel energy resource stored in PC plastic. Hence, it is vital to develop effective and environmentally friendly approaches for the sustainable disposal of PC wastes possibly with energy or chemical recovery.

Thermochemical processes, such as pyrolysis and gasification, offer versatile and promising solutions to convert biomass and plastic wastes into fuels and value-added chemicals, which help address issues on both energy production and waste management. Pyrolysis involves anaerobic thermal decomposition of carbonaceous solids performed for syngas production (with dominating components being H_2 , CO, CO_2 , and light hydrocarbons), condensable vapors (referred as tar or pyrolysis oil), and solid residue (referred as char). In contrast, gasification involves pyrolysis in the presence of mild oxidation using added steam, CO_2 , air, or their mixture to reform the feedstock materials to produce enhanced syngas, while minimizing tar, and char. Even here, pyrolysis is the first step, which is followed by pyrolytic vapor reforming and char gasification to effectively improve the syngas yield [9]. The yields and properties of products from these thermochemical processes are highly dependent on the operation parameters (such as temperature and gasifying agent) and feedstock composition. Typically, lignocellulosic biomass is characterized by the three-dimensional polymerized structure constituting of cellulose, hemicellulose, and lignin, resulting in complex pyrolysis behavior [10]. The abundant oxygenate content in lignocellulosic biomass leads to the formation of reactive oxygenated species such as furan/pyran derivatives and anhydrosugars along with oxygenated radicals such as OH during its pyrolysis [11]. Conversely, plastics degradation proceeds via random-scission mechanism with the pyrolysis products greatly dependent on the monomer structure [12]. The use of plastic materials as feedstock for pyrolysis and gasification offers benefits of feedstock uniformity, high energy density, as well as low ash and moisture contents, which favor sustainable production of syngas with high heating value. However, high-temperature viscous behavior and low thermal conductivity of plastics lead to critical material handling issues. Severe agglomeration of bed materials, blockage of feeding system, and defluidization due to viscous plastic melt were reported in fluidized bed reactors [13,14]. Most recently, co-processing of plastic wastes with biomass has attracted growing attention as it not only provides pathways for simultaneous energy production and waste valorization but also helps to address the operating problems raised by the viscous plastics and supplementing the biomass during its off-seasonal crisis [15,16]. Co-processing of biomass–plastic mixtures was reported to cause nonadditive synergistic behavior compared to those from individual component feedstocks during pyrolysis/gasification [17,18]. Initial studies on steam co-gasification of polyethylene (PE) and wood chips by Ahmed et al. [19] revealed synergistic enhancement of

H_2 and syngas yields. Xue et al. [20] showed that the co-pyrolysis of high-density polyethylene (HDPE) and red oak in a fluidized bed reactor leads to enhanced production of oxygenated compounds such as furan and acids and inhibited formation of char, while the particulates from HDPE blocked the biochar pores as observed by the lowered Brunauer–Emmett–Teller (BET) surface area of the char. Déparrois et al. [21] reported that the H_2 and syngas yields were significantly improved from co-pyrolysis of polystyrene (PS) and paper blends compared to the weighted average values from individual components' pyrolysis and that the blend with PS mass content of 20% provided the highest synergistic enhancement in syngas formation. Burra and Gupta [22] revealed enhanced carbon conversion from co-pyrolysis of different plastic wastes with pinewood, while analysis using the distributed activation energy model showed that the overlap of decomposition temperatures of plastic and biomass was a prerequisite for these thermogravimetric analysis (TGA)-observed synergistic effects.

Although the co-processing of biomass and plastic wastes has received considerable attention in the literature, most available studies were conducted with the combination of biomass and different polyolefins (such as polyethylene (PE), polypropylene (PP), and polystyrene (PS)). Very limited information is available on the co-pyrolysis of biomass and PC with a focus on understanding the synergistic effects. Possible suggestions for the synergistic pathway included enhanced plastic degradation by reactive radicals from biomass decomposition [23,24] and catalytic influence of biomass char on plastic degradation [25]. It is noteworthy that these investigations were all carried out with the evenly mixed biomass–plastic blends. In the co-pyrolysis of certain biomass and plastic mixtures, the intermediates evolved can interact with the two different feedstocks, in addition to the interaction between the volatiles and the feedstock, volatiles and chars, solid feedstocks and chars. All of these interactions contribute to the overall synergy. Thus, understanding their contributions to synergistic effects is necessary. Utilization of evenly mixed feedstocks for co-pyrolysis studies is ill equipped to unravel these intricate interaction pathways and their influence on synergistic product enhancement. This motivated us to systematically investigate the synergistic effects in co-pyrolysis of lignocellulosic biomass and PC wastes.

In the present work, the co-pyrolysis of pinewood and PC was performed in a fixed bed reactor at 900 °C with a focus on the extent of synergistic effects and the possible underlying mechanism. The extent of synergistic effects on syngas evolution, cumulative syngas yield, and char residue yield was quantified via a direct comparison of results from co-pyrolysis of pinewood–polycarbonate mixture with the calculated weighted-averaging values based on the initial feedstock mass fractions from individual pyrolysis. The separated contributions from the catalytic effects of chars from the feedstock components to the overall synergy were evaluated based on the defined feedstock configurations. These results are necessary to realize sustainable and reliable energy production from the increased utilization of lignocellulosic biomass and PC wastes.

2 Experimental

2.1 Materials. Pinewood pellets and bisphenol A polycarbonate were used as the representative lignocellulosic biomass and waste plastics, respectively, to investigate the possible synergistic effects during their co-pyrolysis. The pinewood pellets of around 8 mm (diameter) × 12 mm (length) were obtained from Drax Biomass. Bisphenol A polycarbonate pellets had characteristic size of 2 mm (diameter) × 4 mm (length) with an average molecular weight (M_w) of 45,000 g/mol and were obtained from Sigma-Aldrich. Both pinewood and polycarbonate were dried at 105 °C for 8 h before their use. Table 1 provides the ultimate analyses, proximate analyses, and lower heating values (LHV) of these feedstocks obtained using elemental analyzer (Vario EL cube, Germany), proximate analyzer (UV-02053-00, USA), and rapid calorimeter (5E-KCIII, China) based on China's National Standard

Table 1 Ultimate analyses, proximate analyses, and LHV of pinewood and polycarbonate

	Ultimate analysis (wt%) ^a					Proximate analysis (wt%) ^b				LHV (MJ/kg)
	C	H	N	S	O ^c	Moisture	Ash	Volatile	Fixed carbon	
Pinewood (PW)	48.72	6.52	0.23	0.12	44.41	0.0	0.2	85.6	14.2	17.65
Polycarbonate (PC)	75.31	5.55	0.00	0.03	19.11	0.0	0.0	79.4	20.6	25.51

^aDry ash free basis.

^bDry basis after heating at 105 °C for 8 h.

^cCalculated by difference.

GB/T 31391 [26], GB/T 212 [27], and GB/T 213 [28], respectively, for pinewood. The data for polycarbonate were obtained from the literature as these characteristics in plastic wastes were expected to be uniform [7,29].

2.2 Reactor Facility. Co-pyrolysis of pinewood and polycarbonate were carried out using a lab-scale semi-batch reactor facility consisting of two electrically heated furnaces (gas preheater and pyrolysis reactor), condensers, pump, filter, gas sampling unit, and micro gas chromatograph (micro GC), see Fig. 1. Further details about the facility are given in Refs. [18,19]. Before each experiment, Ar (purity: 99.998%) was used to purge the system to remove any gas residues from a previous run. N₂ (purity: 99.998%) was used as the inert tracer gas for the quantitative analysis of product gases that evolved from pyrolysis. The tests were conducted at the pyrolysis reactor temperature of 900 °C. A quartz cylindrical tube was used to hold the sample that allowed for easy sample introduction and char residue extraction from the pyrolysis reactor. For each experiment, 35 g sample with tailored feedstock configurations was introduced to the pyrolysis reactor at the set-point temperature via a quick disconnect coupling. The electricity consumption of the electric furnace during the

endothermic pyrolysis process was recorded by an electrical meter (EML-2000, Canada).

Product gases from the pyrolysis reactor were passed through ice bath condensers to remove tar and moisture. The dry and tar free gas mixture was analyzed using a micro GC (Agilent 3000A, USA) to determine the molar fractions of N₂, H₂, CO, CO₂, CH₄, C₂H₂, C₂H₄, and C₂H₆ in the evolved product gases with accuracy up to ±0.1%. Sampling bottles were used to collect the samples in case of sampling at shorter times than that needed for the analysis by the GC. The pyrolysis experiments were carried out until 21 min, at which the evolved product gases were negligible. Based on the GC measurements and the known trace gas flowrate (N₂), the mass flowrate and the cumulative yield of each gas component from pyrolysis were determined as widely used in our previous studies [30,31]. All experiments were repeated three times, and the average value was reported here.

The details of tailored feedstock configurations are shown in Fig. 2. The co-pyrolysis cases reported here were performed at 900 °C with the weight ratio of pinewood (PW) to polycarbonate (PC) fixed at 1:1. Cases 1–3 were arranged to quantify the extent of synergistic effects. Specifically, case 1 (denoted as Mix) was the co-pyrolysis case with evenly mixed configuration. Case 2 and Case 3 were the pyrolysis of PW and PC as individual feedstocks, which were employed as the baseline cases to identify the possible synergistic

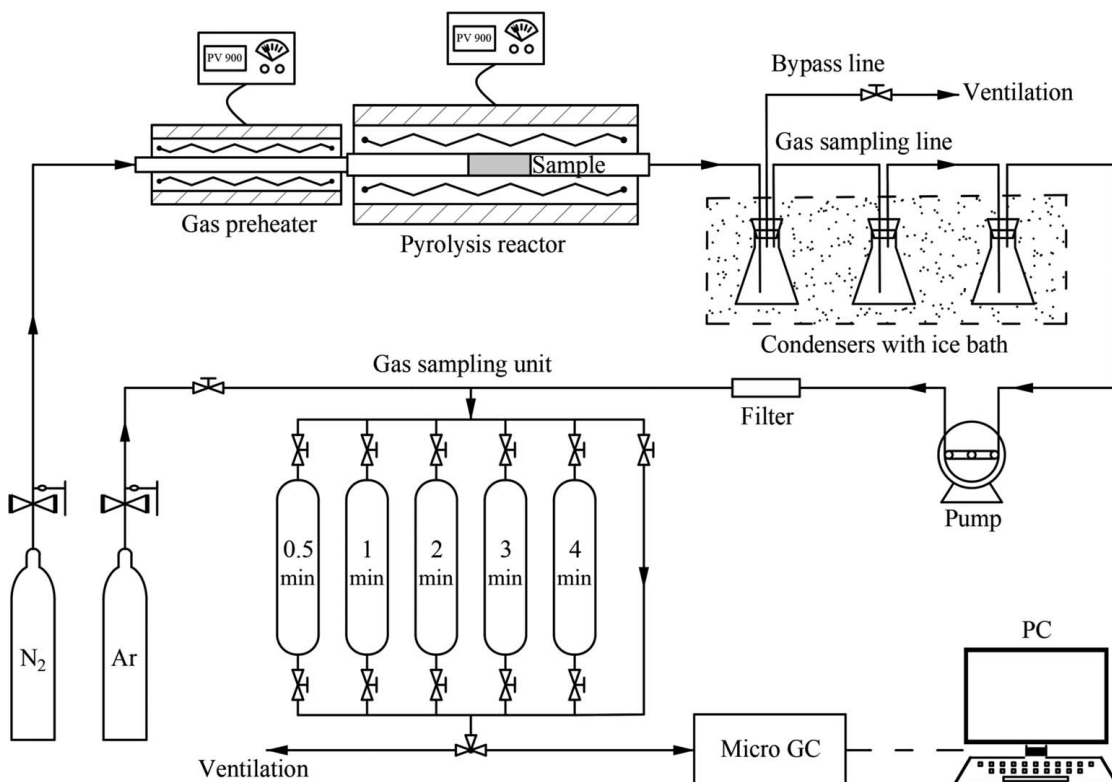


Fig. 1 Schematic diagram of the experimental facility

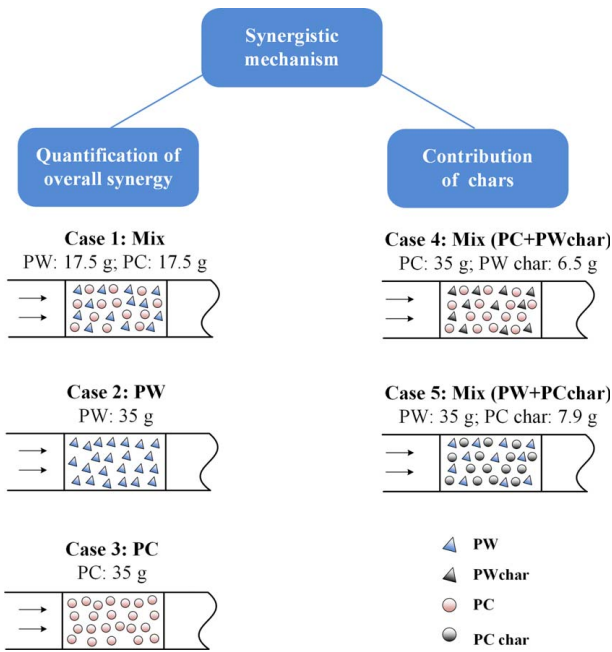


Fig. 2 Tailored feedstock configurations and experiment cases

effects in co-pyrolysis. The extent of synergistic effects then can be evaluated via a direct comparison between the results from co-pyrolysis of PW–PC mixture with the corresponding weighted average values from pyrolysis of individual components, using Eqs. (1) and (2). In these equations, Y_{PW} , Y_{PC} , and Y_{Mix} are the experimental values (gas flowrate and yield, energy yield, char yield, or other parameters) from individual PW pyrolysis, individual PC pyrolysis, and co-pyrolysis of evenly mixed PW–PC mixture, respectively; $Y_{Weighted}$ is the weighted average values based on Eq. (1), α is the mass fraction of PW in the mixed feedstock, and ΔY is the extend of synergistic effects.

$$Y_{Weighted} = \alpha Y_{PW} + (1 - \alpha) Y_{PC} \quad (1)$$

$$\Delta Y = \frac{Y_{Mix} - Y_{Weighted}}{Y_{Weighted}} \quad (2)$$

Cases 4 and 5 were deployed to understand the roles of PW char and PC char in co-pyrolysis. Case 4 involved the pyrolysis of PC in the presence of PW char, and Case 5 considered the pyrolysis of PW in the presence of PC char. These two cases are expected to

provide information on the effect of char from PW and PC on each other's decomposition. Note that char used here was prepared from the individual pyrolysis of PW and PC at 900 °C for 21 min, which was the same condition as that of co-pyrolysis of PW–PC mixture. Moreover, the amount of char used (PW char 6.5 g, PC char 7.9 g) was determined based on the mass ratio of PW to PC at 1:1 after the mass of char was converted to that of original feedstock (PW 35 g, PC 35 g).

3 Results and Discussion

3.1 Quantified Synergistic Effects in Mixture Pyrolysis.

Figure 3(a) shows the mass yield distribution of gas, tar, and char products from co-pyrolysis of PW–PC mixture and individual pyrolysis of PW and PC. High aromatic content and better thermal stability due to the phenolic monomer structure in PC compared to PW resulted in higher tar and char yields but lower gas yield during pyrolysis. The co-pyrolysis of PW and PC led to a noticeable rise in gas yield from 67.6 wt% to 77.2 wt% while decreasing tar (from 11.8 wt% to 7.7 wt%) and char (from 20.6% to 15.1 wt%) yields compared to the weighted values from individual pyrolysis. This result indicates that the synergistic effects in co-pyrolysis of PW and PC not only involved mutual volatiles interactions to occur in gas phase but also included volatiles–solid interactions toward enhanced net conversion of solid feedstock to gases/vapors. Figure 3(b) shows the cumulative mass yields of different gas components from co-pyrolysis and individual pyrolysis. The results show that H_2 and CO yields from co-pyrolysis were enhanced by 33% and 26%, respectively, compared to the weighted average values from individual pyrolysis, while a slight reduction (~6%) in C_nH_m yield was observed in co-pyrolysis. Accordingly, the total syngas yield (considered here as the mixture of H_2 , CO, and C_nH_m) was enhanced by 19% in co-pyrolysis. In addition, cumulative CO_2 yield from co-pyrolysis was similar to the weighted value, which shows the positive outcomes of co-pyrolysis with remarkable enhancement in syngas yield, while the unwanted CO_2 yield remained unchanged. Syngas composition (vol%) from co-pyrolysis and individual pyrolysis is illustrated in Fig. 4. The co-pyrolysis of PW and PC brought a noticeable elevation in H_2 and CO volume fractions but a slight decrease in C_nH_m volume fraction compared to the weighted values, suggesting the improved syngas quality. This improved syngas quality from co-pyrolysis is useful for the clean combustion of syngas for direct energy production and other versatile applications involving synthesis of value-added chemicals.

Overall energy efficiency

$$= \frac{E_{output, syngas}}{E_{input, feedstock} + E_{input, electricity}} \times 100\% \quad (3)$$

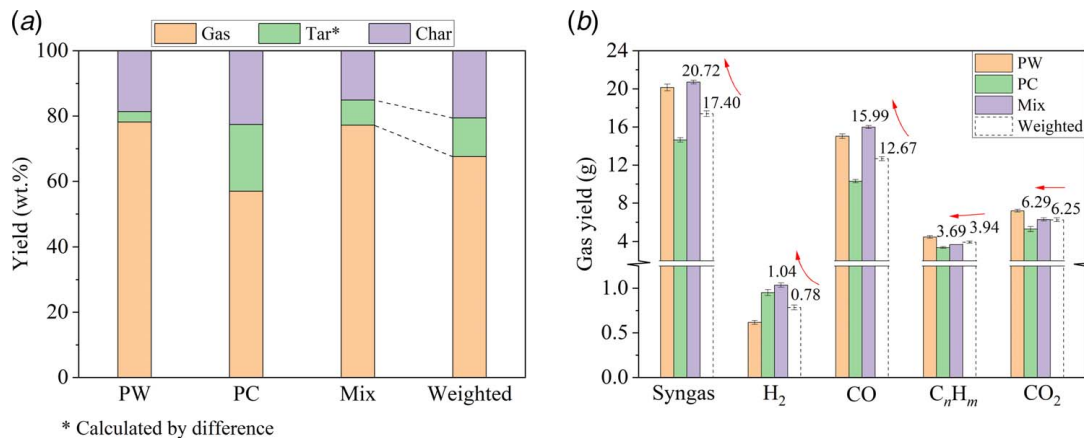


Fig. 3 (a) Mass distribution of gas, tar, and char products and (b) cumulative yields of different gas components from co-pyrolysis of PW–PC mixture and individual pyrolysis of PW and PC

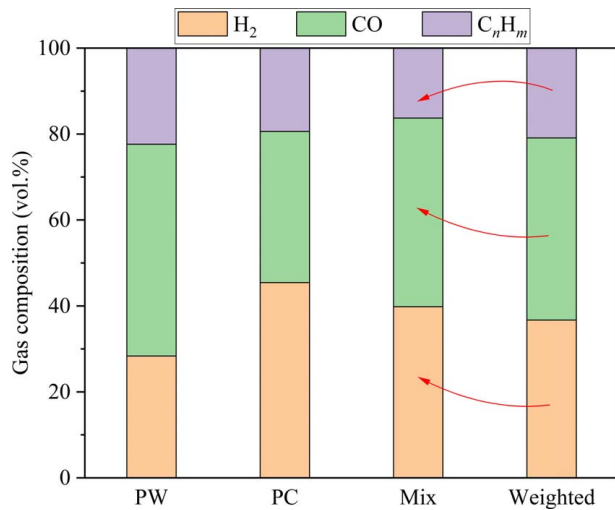
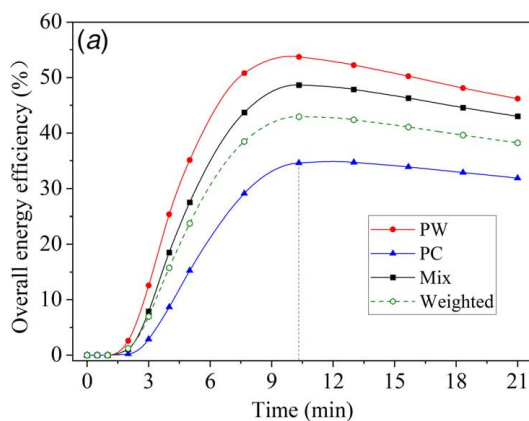


Fig. 4 Cumulative syngas composition from co-pyrolysis of PW–PC mixture and individual pyrolysis of PW and PC

Figure 5(a) shows the comparison of overall energy efficiency between co-pyrolysis and individual pyrolysis of PW and PC. Overall energy efficiency considered here was defined as the ratio of energy extracted as calorific content of syngas to the overall energy spent in its production [31], see Eq. (3), where $E_{\text{output, syngas}}$ refers to the calorific content of the evolved syngas, $E_{\text{input, feedstock}}$ refers to the energy input from calorific content in original feedstock, and $E_{\text{input, electricity}}$ refers to the energy input from electricity consumption by the heating furnace to support the endothermic pyrolysis. This parameter provides important information for evaluating the feasibility of co-pyrolysis and individual pyrolysis in energy recovery aspect. As shown in Fig. 5(a), the overall energy efficiency increased steeply in the initial stage (0–10.3 min) and then gradually decreased as the reaction time prolonged for all the cases examined here. A rapid increase in the initial stage was due to intense syngas evolution. This was then followed by a gradual decline because the feedstock reached nearly complete conversion, while the energy input (i.e., electricity consumption) was still needed to cover the heat losses from the pyrolysis reactor. Figure 5(a) also shows the overall energy efficiency reached peak value at the reaction time of 10.3 min. This result can be helpful in providing reactor design requirements for determining the optimal feedstock residence time without losing energy efficiency. The co-pyrolysis of PW and PC led to a 5.7% point increase in overall energy efficiency compared to the weighted value, because the synergistic effects in co-pyrolysis of



PW and PC resulted in a remarkable enhancement in syngas energy, while the electricity consumption remained almost unchanged (see Fig. 5(b)). This significant elevation in energy efficiency signifies the need for co-pyrolysis for energy production.

3.2 Effect of Feedstock Chars on Synergistic Interaction.

The contributions of PW char and PC char toward the observed synergistic effects in co-pyrolysis of PW–PC mixture were evaluated with two specific pyrolysis scenarios of pyrolysis of PC in the presence of PW char (denoted as Mix (PC + PWchar)) and pyrolysis of PW in the presence of PC char (denoted as Mix (PW + PCchar)). In the case of co-pyrolysis of PW–PC mixture, PW attained charring stage in parallel with the proceeding of PC degradation, while by the time PC char was formed, PW had reached nearly complete conversion. Hence, the interactions between PW char and PC melt were expected to be more pronounced than interactions between PC char of PW feedstock in co-pyrolysis of PW–PC mixture due to the improved overlap. Even though the overlap between PC char and PW may be insignificant in co-pyrolysis, the pyrolysis case of PW in the presence of PC char (Mix (PW + PCchar)) was still designed to verify whether PC char had some influences on PW decomposition.

Figure 6 shows the evolution of the flowrates of (a) H₂, (b) CO, (c) C_nH_m, and (d) CO₂ from pyrolysis of PC, PW char, and PC + PW char mixture. The results showed that PW char alone did not yield any gas product, but the addition of PW char in PC remarkably promoted H₂ and CO flowrates but decreased C_nH_m flowrate from PC. The cumulative H₂ yield increased from 0.95 g for pure PC pyrolysis to 1.08 g for pyrolysis of PC + PW char mixture. Similar enhancement in CO yield from 10.31 g to 11.68 g and decline in C_nH_m yield from 3.38 g to 3.07 g were observed in pyrolysis of PC + PW char mixture. These results indicated that the addition of PW char significantly affected PC decomposition. The changes in gas yields presented here can be interpreted by the following pathways. PC pyrolysis yielded a wide range of phenolic intermediates with hydroxyl groups (C_{aromatic}–OH) and ester groups (C_{aromatic}–O–C) bonded to the benzene ring. Based on the bond dissociation energies in the order of C_{aromatic}–O–C < C_{aromatic}–OC < C_{aromatic}–OH [32,33], during PC pyrolysis, the cleavage of C_{aromatic}–O–C bond tended to occur first, resulting in the release of aliphatic hydrocarbon side chains, followed by cracking reactions to form light hydrocarbons. While in the case of pyrolysis of PW + PC char mixture, PC degraded in the presence of abundant alkali and alkaline earth metals (AAEMs) from PW char. It is reported that AAEMs in biomass char and the porous carbon in the char had catalytic effect in deoxygenation of phenolic intermediates [34], thereby enhancing the cleavage of C_{aromatic}–OC and C_{aromatic}–OH bonds to form more oxygen-containing groups, followed by

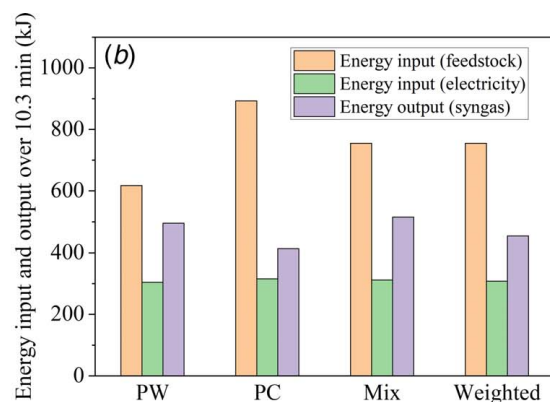


Fig. 5 Comparison of (a) overall energy efficiency and (b) energy input and output over 10.3 min between co-pyrolysis of PW–PC mixture and individual pyrolysis of PW and PC

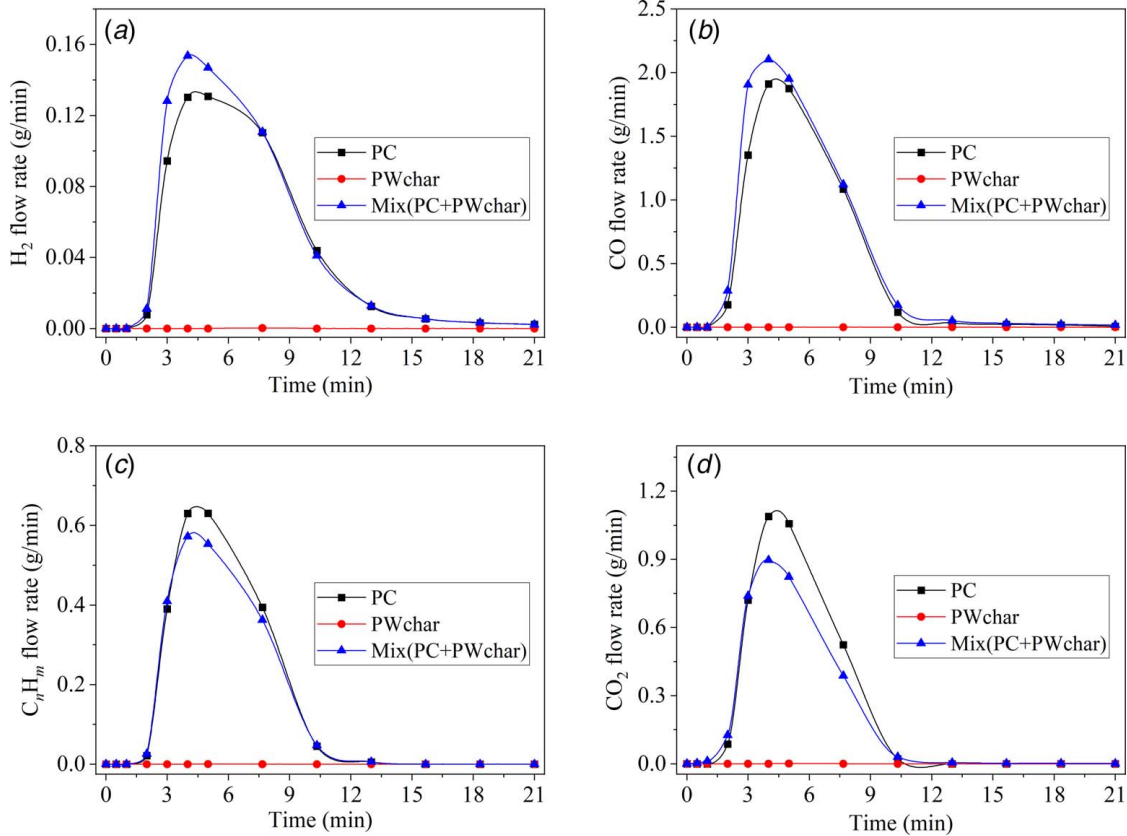


Fig. 6 Evolution of the flowrates of (a) H_2 , (b) CO, (c) C_nH_m , and (d) CO_2 from pyrolysis of PC, PW char, and PC + PW char mixture

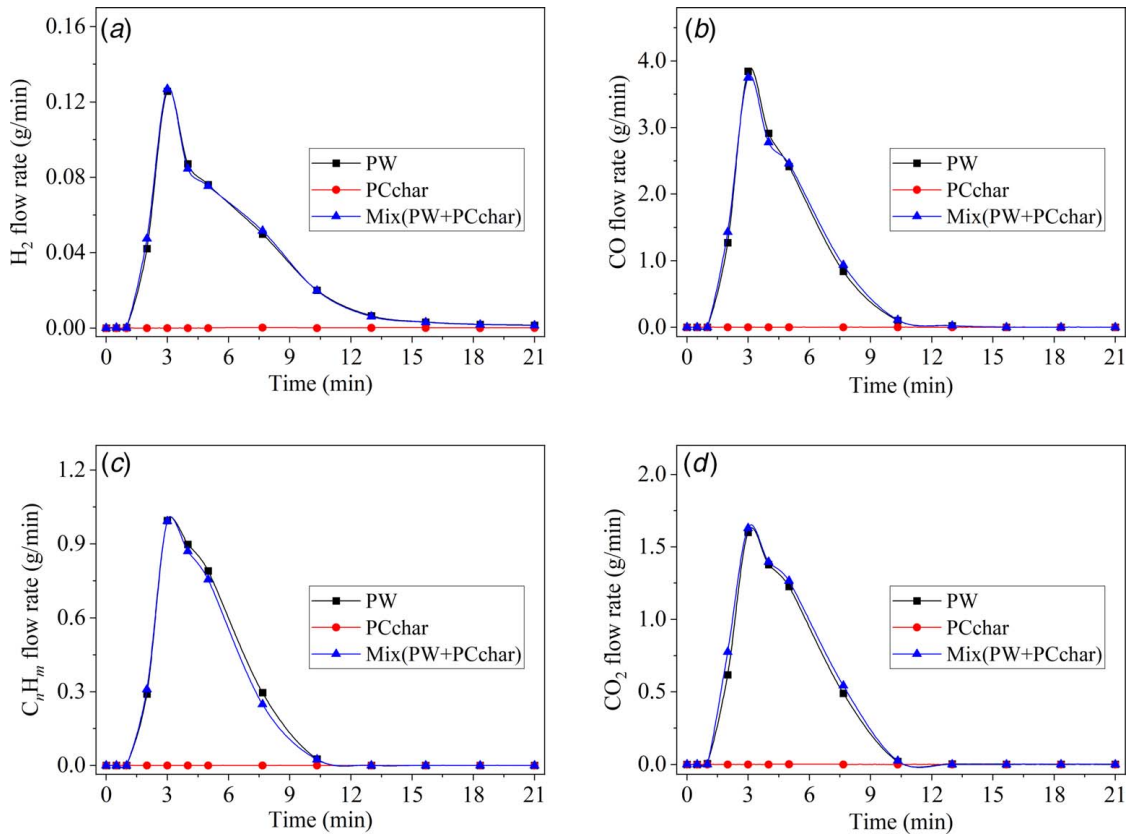


Fig. 7 Evolution of the flowrates of (a) H_2 , (b) CO, (c) C_nH_m , and (d) CO_2 from pyrolysis of PW, PC char, and PW + PC char mixture

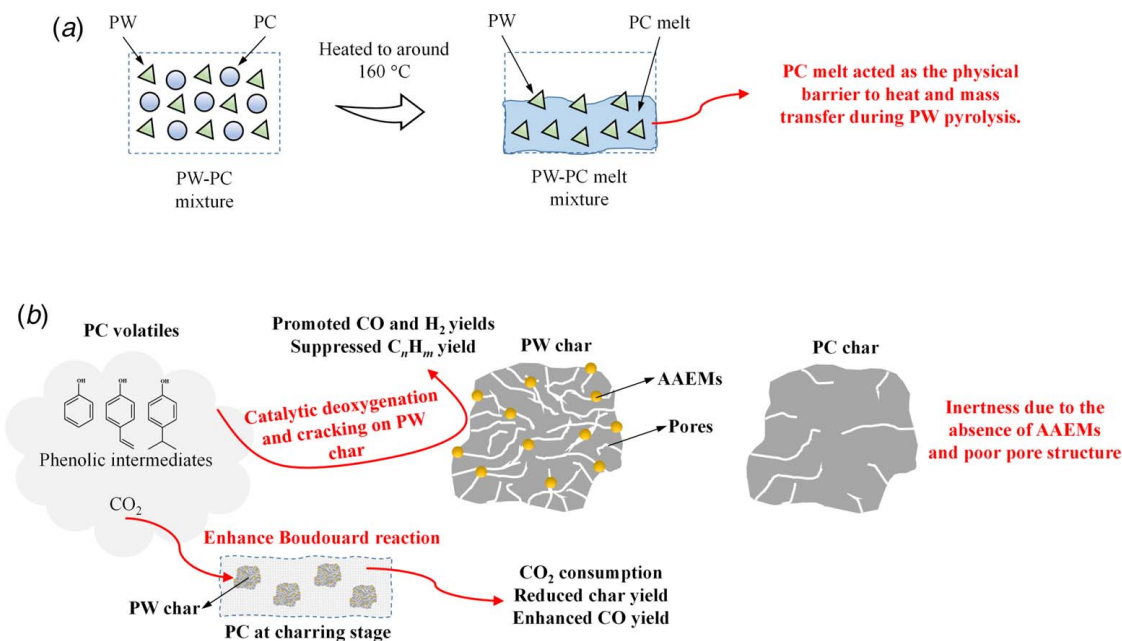


Fig. 8 Tested synergistic pathways in co-pyrolysis of PW and PC: (a) feedstock–feedstock physical interactions and (b) catalytic effects of PW char and PC char

decarbonylation and cracking reactions to yield more CO and H₂ at the expense of declined C_nH_m yield. In addition, AAEMs and porous carbon in biomass char catalyzed the cracking of PC oligomers and primary pyrolysis products [35], contributing to enhanced H₂ formation. Wang et al. [36] reported that the inherent AAEMs in biomass had negative influence on yields of both light hydrocarbons and aromatic hydrocarbons from pyrolysis. Antonakou et al. [5] found that employing basic metal oxides (CaO and MgO) as catalysts for PC pyrolysis enhanced the formation of low-molecular-weight compounds and the yields of H₂ and CO were significantly promoted. The catalytic effect of AAEM on Boudouard reaction has been reported in many gasification investigations to promote char reactivity [37]. In our case, char residue from pyrolysis of PC + PW char mixture was 13.4 g, which was lower than the calculated value 14.4 g (assuming PW char had no interaction with PC during pyrolysis), confirming that the presence of AAEM in PW char facilitated the Boudouard reaction causing decreased CO₂ and char yields.

Figure 7 shows the evolution of the flowrates of (a) H₂, (b) CO, (c) C_nH_m, and (d) CO₂ from pyrolysis of PW, PC char, and PW + PC char mixture. It can be observed that the flowrates of all gas components from pyrolysis of PW + PC char mixture almost coincided with the results from pure PW pyrolysis, suggesting the negligible effect of PC char on PW decomposition. The inertness of PC char for PW pyrolysis presented here was mainly attributed to the lack of catalytic activity of PC char toward deoxygenation, cracking, and Boudouard reaction pathways due to the absence of AAEMs and active porosity as shown in our previous study that the BET surface area of char from pinewood pyrolysis was approximately threefold higher than that from polymer pyrolysis [17]. The relatively lower surface area of PC char led to insufficient active sites to support the interactions between PC char and PW that lead to negligible effect of PC char on PW pyrolysis. The results shown here reveals that PW char contributed to the synergistic effects in co-pyrolysis of PW and PC, while PC char can be considered as an inert material during co-pyrolysis process.

Based on the aforementioned analyses, synergistic mechanism and some of the possible synergistic pathways in co-pyrolysis of PW and PC are illustrated in Fig. 8, including feedstock–feedstock physical interactions and catalytic effects of PW char and PC char.

When PW–PC mixture was heated to around 160 °C (over PC’s glass transition temperature), PC transitioned to viscous melt-phase

due to its thermoplasticity. PW pellets in the mixture were then immersed or incorporated in the PC melt. The formed PC melt acted as a physical barrier, which hindered the transport of evolved PW volatiles out of the mixture and impeded the heat input to support the endothermic pyrolysis process. This physical interaction between PW pellets and PC melt resulted in delayed syngas evolution in co-pyrolysis of PW–PC mixture compared to the co-pyrolysis with separated feedstock configurations.

Figure 8(b) shows the catalytic effects of PW char and PC char in co-pyrolysis of PW and PC. PW char contained abundant AAEMs and developed porous structure, which facilitated the deoxygenation and cracking of phenolic intermediates to generate more CO and H₂ but less C_nH_m. Moreover, the abundant AAEMs in PW char catalytically favored the Boudouard reaction, resulting in CO₂ consumption and subsequently enhancing the CO yield. However, PC char was characterized with no AAEMs and poor porous structure, which showed no catalytic effect and can be considered as an inert material during the co-pyrolysis process.

4 Conclusions

Co-pyrolysis of pinewood and polycarbonate using tailored feedstock configurations was examined to determine the extent of synergistic effects and gain enhanced understanding of the separate contributions of chars to the overall synergy. The results showed that the co-pyrolysis of pinewood and polycarbonate strongly affected mass distribution of gas, tar, and char products due to the presence of synergistic effects. H₂ yield, CO yield, and total syngas yield from co-pyrolysis were enhanced by 33%, 26%, and 19%, respectively, compared to the weighted average values from pyrolysis of individual components, while char and tar yields remarkably decreased in co-pyrolysis. Co-pyrolysis of these two feedstocks also showed enhanced syngas quality and improved overall energy efficiency, which signified the important advantages of co-utilization of biomass and plastic waste for energy production.

Co-pyrolysis of polycarbonate in the presence of pinewood char indicated that the developed porous structure and considerable AAEMs in pinewood char catalytically facilitated the deoxygenation and cracking of phenolic intermediates in polycarbonate volatiles to yield more CO and H₂, in parallel with catalytically enhanced Boudouard reaction leading to CO₂ consumption and

decreased char yield. However, polycarbonate char showed no influence on pinewood pyrolysis mainly due to its poor porous structure and absence of AAEMs.

Acknowledgment

This research was supported by Office of Naval Research and their support is gratefully acknowledged. The support provided to the authors (Xuan Liu, Zhiwei Wang, and Jinhui Li) from China Scholarship Council (CSC201906280344) is gratefully acknowledged. The support provided to the author (K.G. Burra) by Ann G. Wylie Fellowship is gratefully acknowledged.

Conflict of Interest

There are no conflicts of interest.

Data Availability Statement

The datasets generated and supporting the findings of this article are obtainable from the corresponding author upon reasonable request. The authors attest that all data for this study are included in the paper. Data provided by a third party listed in Acknowledgment. No data, models, or code were generated or used for this paper.

References

- [1] Dudley, R., and BP Energy Outlook, 2014, "BP Energy Outlook 2019 Edition the Energy Outlook Explores the Forces Shaping the Global Energy Transition Out to 2040 and the Key Uncertainties Surrounding That," Energy Outlook, February 15, 2019, pp. 1–73, <https://www.bp.com/en/global/corporate/news-and-insights/pres-releases/bp-energy-outlook-2019.html>.
- [2] Sheldon, R. A., 2014, "Green and Sustainable Manufacture of Chemicals From Biomass: State of the art," *Green Chem.*, **16**(3), pp. 950–963.
- [3] Chan, F. L., and Tanksale, A., 2014, "Review of Recent Developments in Ni-Based Catalysts for Biomass Gasification," *Renew. Sustain. Energy Rev.*, **38**(1), pp. 428–438.
- [4] Bai, B., Liu, Y., Meng, X., Liu, C., Zhang, H., Zhang, W., and Jin, H., 2020, "Experimental Investigation on Gasification Characteristics of Polycarbonate (PC) Microplastics in Supercritical Water," *J. Energy Inst.*, **93**(2), pp. 624–633.
- [5] Antonakou, E. V., Kalogiannis, K. G., Stefanidis, S. D., Karakoulia, S. A., Triantafyllidis, K. S., Lappas, A. A., and Achilias, D. S., 2014, "Catalytic and Thermal Pyrolysis of Polycarbonate in a Fixed-Bed Reactor: The Effect of Catalysts on Products Yields and Composition," *Polym. Degrad. Stab.*, **110**(12), pp. 482–491.
- [6] Do, T., Baral, E. R., and Kim, J. G., 2018, "Chemical Recycling of Poly(Bisphenol A Carbonate): 1,5,7-Triazabicyclo[4.4.0]-dec-5-ene Catalyzed Alcoholysis for Highly Efficient Bisphenol A and Organic Carbonate Recovery," *Polymer*, **143**, pp. 106–114.
- [7] Wang, J., Jiang, J., Meng, X., Li, M., Wang, X., Pang, S., Wang, K., Sun, Y., Zhong, Z., Ruan, R., and Ragauskas, A. J., 2020, "Promoting Aromatic Hydrocarbon Formation via Catalytic Pyrolysis of Polycarbonate Wastes Over Fe- and Ce-Loaded Aluminum Oxide Catalysts," *Environ. Sci. Technol.*, **54**(13), pp. 8390–8400.
- [8] Arulmozhiraja, S., Coote, M. L., Kitahara, Y., Juhász, M., and Fujii, T., 2011, "Is the Bisphenol A Radical Formed in the Pyrolysis of Polycarbonate?," *J. Phys. Chem. A.*, **115**(19), pp. 4874–4881.
- [9] Wang, Z., Burra, K. G., Lei, T., and Gupta, A. K., 2019, "Co-Gasification Characteristics of Waste Tire and Pine Bark Mixtures in CO₂ Atmosphere," *Fuel*, **257**, p. 116025.
- [10] Dai, G., Zhu, Y., Yang, J., Pan, Y., Wang, G., Reubroycharoen, P., and Wang, S., 2019, "Mechanism Study on the Pyrolysis of the Typical Ether Linkages in Biomass," *Fuel*, **249**, pp. 146–153.
- [11] Wang, S., Dai, G., Yang, H., and Luo, Z., 2017, "Lignocellulosic Biomass Pyrolysis Mechanism: A State-of-the-Art Review," *Prog. Energy Combust. Sci.*, **62**, pp. 33–86.
- [12] Lopez, G., Artetxe, M., Amutio, M., Alvarez, J., Bilbao, J., and Olazar, M., 2018, "Recent Advances in the Gasification of Waste Plastics. A Critical Overview," *Renew. Sustain. Energy Rev.*, **82**(Part 1), pp. 576–596.
- [13] Lopez, G., Erkiaga, A., Amutio, M., Bilbao, J., and Olazar, M., 2015, "Effect of Polyethylene Co-Feeding in the Steam Gasification of Biomass in a Conical Spouted Bed Reactor," *Fuel*, **153**, pp. 393–401.
- [14] Robinson, T., Bronson, B., Gogolek, P., and Mehrani, P., 2016, "Comparison of the Air-Blown Bubbling Fluidized bed Gasification of Wood and Wood-PET Pellets," *Fuel*, **178**, pp. 263–271.
- [15] Pinto, F., André, R., Miranda, M., Neves, D., Varela, F., and Santos, J., 2016, "Effect of Gasification Agent on Co-Gasification of Rice Production Wastes Mixtures," *Fuel*, **180**, pp. 407–416.
- [16] Brachi, P., Chiron, R., Miccio, F., Miccio, M., Picarelli, A., and Ruoppolo, G., 2014, "Fluidized Bed Co-Gasification of Biomass and Polymeric Wastes for a Flexible End-Use of the Syngas: Focus on Bio-Methanol," *Fuel*, **128**, pp. 88–98.
- [17] Wang, Z., Burra, K. G., Zhang, M., Li, X., Policella, M., Lei, T., and Gupta, A. K., 2020, "Co-Pyrolysis of Waste Tire and Pine Bark for Syngas and Char Production," *Fuel*, **274**, pp. 117878.
- [18] Burra, K. G., and Gupta, A. K., 2018, "Synergistic Effects in Steam Gasification of Combined Biomass and Plastic Waste Mixtures," *Appl. Energy*, **211**, pp. 230–236.
- [19] Ahmed, I. I., Nipattummakul, N., and Gupta, A. K., 2011, "Characteristics of Syngas From Co-Gasification of Polyethylene and Woodchips," *Appl. Energy*, **88**(1), pp. 165–174.
- [20] Xue, Y., Zhou, S., Brown, R. C., Kelkar, A., and Bai, X., 2015, "Fast Pyrolysis of Biomass and Waste Plastic in a Fluidized Bed Reactor," *Fuel*, **156**, pp. 40–46.
- [21] Déparrois, N., Singh, P., Burra, K. G., and Gupta, A. K., 2019, "Syngas Production From Co-Pyrolysis and Co-Gasification of Polystyrene and Paper With CO₂," *Appl. Energy*, **246**, pp. 1–10.
- [22] Burra, K. G., and Gupta, A. K., 2018, "Kinetics of Synergistic Effects in Co-Pyrolysis of Biomass With Plastic Wastes," *Appl. Energy*, **220**, pp. 408–418.
- [23] Wu, C., and Williams, P. T., 2010, "Pyrolysis–Gasification of Plastics, Mixed Plastics and Real-World Plastic Waste With and Without Ni–Mg–Al Catalyst," *Fuel*, **89**(10), pp. 3022–3032.
- [24] Alvarez, J., Kumagai, S., Wu, C., Yoshioka, T., Bilbao, J., Olazar, M., and Williams, P. T., 2014, "Hydrogen Production From Biomass and Plastic Mixtures by Pyrolysis-Gasification," *Int. J. Hydrogen Energy*, **39**(21), pp. 10883–10891.
- [25] Jakab, E., Várhegyi, G., and Faix, O., 2000, "Thermal Decomposition of Polypropylene in the Presence of Wood-Derived Materials," *J. Anal. Appl. Pyrolysis*, **56**(2), pp. 273–285.
- [26] China National Standards and Codes: GB/T 31391-2015, 2015, *Ultimate Analysis of Coal*, Standardization Administration of the People's Republic of China, Beijing.
- [27] China National Standards and Codes: GB/T 212-2008, 2008, *Proximate Analysis of Coal*, Standardization Administration of the People's Republic of China, Beijing.
- [28] China National Standards and Codes: GB/T 213-2008, 2008, *Determination of Calorific Value of Coal*, Standardization Administration of the People's Republic of China, Beijing.
- [29] Othman, N., Basri, N. E. A., and Yunus, M. N. M., 2008, "Determination of Physical and Chemical Characteristics of Electronic Plastic Waste (Ep-Waste) Resin Using Proximate and Ultimate Analysis Method," *ICCBT*, **1**(1), pp. 169–180.
- [30] Liu, X., Burra, K. G., Wang, Z., Li, J., Che, D., and Gupta, A. K., 2020, "On Deconvolution for Understanding Synergistic Effects in Co-Pyrolysis of Pinewood and Polypropylene," *Appl. Energy*, **279**, p. 115811.
- [31] Wang, Z., Liu, X., Burra, K. G., Li, J., Zhang, M., Lei, T., and Gupta, A. K., 2021, "Towards Enhanced Catalytic Reactivity in CO₂-Assisted Gasification of Polypropylene," *Fuel*, **284**, p. 119076.
- [32] Zhang, J., Sun, J., and Wang, Y., 2020, "Recent Advances in the Selective Catalytic Hydrodeoxygenation of Lignin-Derived Oxygenates to Arenes," *Green Chem.*, **22**(4), pp. 1072–1098.
- [33] Prasomsri, T., Shetty, M., Murugappan, K., and Román-Leshkov, Y., 2014, "Insights Into the Catalytic Activity and Surface Modification of MoO₃ During the Hydrodeoxygenation of Lignin-Derived Model Compounds Into Aromatic Hydrocarbons Under Low Hydrogen Pressures," *Energy Environ. Sci.*, **7**(8), pp. 2660–2669.
- [34] Guo, X., Wang, W., Wu, K., Huang, Y., Shi, Q., and Yang, Y., 2019, "Preparation of Fe Promoted MoS₂ Catalysts for the Hydrodeoxygenation of p-Cresol as a Model Compound of Lignin-Derived Bio-Oil," *Biomass Bioenergy*, **125**, pp. 34–40.
- [35] Persson, H., and Yang, W., 2019, "Catalytic Pyrolysis of Demineralized Lignocellulosic Biomass," *Fuel*, **252**, pp. 200–209.
- [36] Wang, K., Zhang, J., Shanks, B. H., and Brown, R. C., 2015, "The Deleterious Effect of Inorganic Salts on Hydrocarbon Yields From Catalytic Pyrolysis of Lignocellulosic Biomass and Its Mitigation," *Appl. Energy*, **148**, pp. 115–120.
- [37] Lahijani, P., Zainal, Z. A., Mohammadi, M., and Mohamed, A. R., 2015, "Conversion of the Greenhouse Gas CO₂ to the Fuel gas CO via the Boudouard Reaction: A Review," *Renew. Sustain. Energy Rev.*, **41**, pp. 615–632.